Global Change Biology (2003) **9,** 1051–1065

The annual carbon budget of a French pine forest (*Pinus pinaster*) following harvest

S. KOWALSKI*, M. SARTORE*, R. BURLETT*, P. BERBIGIER† and D. LOUSTAU*
**INRA Bordeaux – Cestas, Laboratoire Ecophysiologie et Nutrition, Recherches Forestières, Domaine de l'Hermitage, Pierroton, 69, route d'Arcachon, 33612 Gazinet, France, †INRA Bioclimatologie, BP 81, F-33883 Villenave d'Ornon, France*

Abstract

Eddy covariance measurements of net ecosystem exchange (NEE) of carbon dioxide and sensible and latent heat have operated since clear felling of a 50-year old maritime pine stand in Les Landes, in Southwestern France. Turbulent fluxes from the closed-path system are computed via different methodologies, including those recommended from EUROFLUX (Adv. Ecol. Res. 30 (2000) 113; Agric. Forest Meteorol. 107 (2001a, b) 43 and 71), and sensitivity analysis demonstrates the merit of post-processing for accurate flux calculation. Footprint modeling, energy balance closure, and empirical modeling corroborate the eddy flux measurements, indicating best reliability in the daytime.

The ecosystem, a net source of atmospheric CO_2, is capable of fixing carbon during fair weather during any season due to the abundance of re-growing species (mostly grass), formerly from the understorey. Annual carbon loss of 200–340 $g\,m^{-2}$ depends on the period chosen, with inter-annual variability evident during the 18-month measurement period and apparently related to available light. Empirical models, with weekly photosynthetic parameters corresponding to seasonal vegetation and respiration depending on soil temperature, fit the data well and allow partitioning of annual NEE into GPP and TER components. Comparison with a similar nearby mature forest (Agric. Forest Meteorol. 108 (2001) 183) indicates that clear-cutting reduces GPP by two thirds but TER by only one third, transforming a strong forest sink into a source of CO_2. Likewise, the loss of 50% of evapotranspiration (by the trees) leads to increased temperatures and thus reduced net radiation (by one third), and a 50% increase in sensible heat loss by the clear cut.

Keywords: eddy covariance, forest carbon cycle, gross primary production (GPP), harvest disturbance, net ecosystem exchange (NEE), total ecosystem respiration (TER)

Received 31 May 2002; revised version received 8 September 2002 and accepted 22 January 2003

Introduction

The role of forests at different development stages following disturbance is a major source of uncertainty in assessing the terrestrial carbon cycle (Geider *et al*., 2002). While direct measurements of annual NEE have shown that mature, growing forests are carbon sinks (Valentini *et al*., 2000; Baldocchi *et al*., 2001), large forest areas of are recovering from the effects of perturbations and their carbon and energy balances are not well documented. In many countries, management represents the main forest disturbance. If forests are to be managed for optimal carbon sequestration, the evolution of carbon exchange processes over the entire forest cycle must be understood, and the period immediately following cutting is crucial.

Because forest soils are vast carbon reservoirs (Post & Kwon, 2000), disturbances to upper soil layers potentially can transform an ecosystem sink into a source (Janssens *et al*., 2001). Presumably, decomposition of accumulated stocks (harvest residues, root systems, humus and soil organic matter) dominates the forest carbon balance after cutting, and the ecosystem remains a source for some period. The recovery time before net annual carbon

Correspondence: D. Loustau, INRA Bordeaux – Cestas, Laboratoire Ecophysiologie et Nutrition, Recherches Forestières, Domaine de l'Hermitage, Pierroton, 69, route d'Arcachon, 33612 Gazinet, France, fax +33 5 56 68 05 46, e-mail: denis@pierroton.inra.fr

fixation resumes may vary from years to decades depending on climate, soil type, and management practices (Law *et al*., 2001). Stands subjected to thinning or poor soil conditions leave light for understorey growth, even prior to harvest. When left during cutting, biodiverse re-growth originating in the understorey may contribute to gross primary production (GPP) almost immediately.

'Les Landes de Gascogne' in southwest France is one of Europe's largest and most intensively managed forests, and is typified by a flourishing understorey. More than a million hectares (Porté, 1999) of mostly maritime pine (*Pinus pinaster*) have been sewn or planted in nutrient-poor, sandy soil. Stands are thinned regularly, produce relatively little needle area even when mature, and allow dense population by ferns (*Pteridium aquilinum*) in mesic soils, and grass (*Molinia coerulea*) where the water table is high enough to maintain soil moisture. The typical rotation period is 50 years, ending in clear-cutting, tilling, and re-planting. Direct NEE measurements show that one 30-year-old-pine/grass ecosystem removes nearly 600 g m^{-2} of atmospheric carbon per year (Berbigier *et al*., 2001).

In this paper, as part of the CARBOAGE project (European Union contract ENV4-CT97-0577), we investigate the carbon, energy and water balances of a forest stand in Les Landes immediately after clear-cutting. While forest practices aimed at site preparation and regeneration are delayed for some years, we focus on the stage characterized by re-growth of natural vegetation and decomposition of harvest residues and accumulated carbon stocks. Eighteen months of eddy covariance NEE measurements are complimented by meteorological and soil measurements to explain processes driving the fluxes, namely photosynthesis and respiration. The micrometeorological estimates are substantiated via empirical modeling, soil CO_2 efflux measurements, footprint modeling (Schmid, 1994), and surface energy budget analysis. The clear-cut ecosystem is a source of atmospheric carbon on an annual basis, on the same order of magnitude as the sink represented by mature forests, and partitions available energy differently from forest.

Materials and methods

The experimental site at Bilos

The ecosystem (44°29′43″N, 0°57′09″W; 38 m a.s.l.) is a quasi-rectangular (1000 × 600 m^2) parcel, owned by the commune of Salles and managed by the National Forest Office. In December 1999, cutting of the 50-year-old stand began with one quarter (15 ha) but is delayed and still pending due to a windstorm that felled several years' harvest in Les Landes. Vegetation is mainly grasses (graminae), heather and gorse, with sparse fern and pine saplings below 3-m (see Appendix). Heaps of dead branches cover significant parts of the ecosystem. Total aboveground biomass (July, considered seasonal peaks) is given in Table 1. From biomass, the maximum LAI of the graminae was estimated in 2000 and 2001 at 1.9 ± 1.1 and 1.6 ± 1, respectively. The LAI of other vegetation groups may be estimated roughly at 0.5, most relevant during winter senescence of the graminae. The well-developed moss layer is not continuous.

Table 1 Peak values of total aboveground biomass in 2000 and 2001 for the main vegetation groups in the clear-cut (kg m^{-2})

	Graminae	Heather	Pine	Gorse	Fern
2000	1.6	3	NA	0.52	NA
2001	1.3	2.9	0.5	0.58	0.24

The landscape is a very flat coastal plain with drainage ditches. An agricultural field, used for corn and carrots, borders the clear-cut to the North. The other borders are mature maritime pine forest, with significant wind throw to the East and West; the fetch is approximately 200 m in every direction. The soil is a sandy podzol lying over a hard iron pan at ca. 70 cm. Groundwater usually is near the surface in winter and below the pan during summer. The pine saplings within the regenerating clear-cut have needle nitrogen (1.56 g m^{-2}) and phosphorus (0.09 g m^{-2}) content (per unit surface area) similar to those found in stands of various ages growing in Les Landes (January 2000 and 2001, data not presented). The climate is temperate-maritime, with an annual mean temperature of 12.8 °C and 930 mm of precipitation, falling mostly in winter (1960–1990 averages from nearby Mérignac and St Symphorine MétéoFrance meteorological stations).

Eddy covariance measurements

The closed-path eddy covariance measurement system was installed in the center of the clear-cut in late April 2000. A 6-m, vertical aluminum mast, planted ca. 50-cm in the soil, supports the EDISOL system (Moncrieff *et al*., 1997) with sonic anemometer and filtered air inlet. The measurement height is 6.39 m, and the air intake is 20 cm (horizontal) from the center of the anemometer transducers. A Solent anemometer (Gill model 1012R3, UK) measures 3-D winds and surrogate temperature at 20 Hz. Molar fractions of CO_2 and H_2O are measured with an infrared LI-6262 gas analyzer (IRGA, LI-COR, USA), which converts ranges of 300–500 μmol mol^{-1} CO_2 and 0–30 mmol mol^{-1} H_2O (absolute mode) to 0–5000 mV analog signals for the anemometer. A microcomputer communicates with the anemometer via RS-232 to store raw data, which are collected onto Zip drives (Iomega, USA) and written to compact disk.

For gas sampling, a 12-V pump (N811 KNDC, KNF Neuberger, USA) draws air at 5.0 L min^{-1} (controlled mass flow) through a 1.0-μm filter (Gelman Acro 50-4258, USA; changed weekly) and into a 7-m Dekabon tube (6.3 mm inner diameter; Saint Gobain, Belgium). The IRGA was kept dry by a coalescing filter (Ballston A944-DX-BSPT, USA) until mains power installation allowed heating of the intake tube in August 2001. The IRGA reference chamber is fed nitrogen at 0.05 L min^{-1}. Seasonal calibrations confirm that the IRGA span drift is negligible.

Ecosystem and climatic measurements

Meteorological and soil sensors, installed in the summer of 2000, are sampled every 10 s (except soil moisture) and stored as half-hour means (Campbell CR23X, USA). Meteorological measurements at 4 m on the mast include air temperature and relative humidity (HMP45C, Vaisala, Finland), wind speed (A100L2, Vector Instruments, UK), downward solar radiation (SKS 1110, Skye Instruments, UK), net radiation (NR-Lite, Kipp & Zonen, The Netherlands), and photosynthetic photon flux density (PPFD, SKP 215, Skye Instruments, UK). Precipitation (ARG100, Environ. Meas., USA) and atmospheric pressure (PTB101B, Vaisala, Finland) are measured on the ground. Underground, two self-calibrating plates (Hukseflux HFP01SC, The Netherlands) measure heat flux at 4 cm under grassy areas, and thermocouples measure temperature at 5 and 10 cm.

Soil moisture is characterized via reflectometry probes. A portable time domain reflectometry (TDR) system (Trase, USA) was deployed from summer 2000 to spring 2001 along two orthogonal, 100-m transects intersecting at the mast. Twenty-cm probes were inserted in the soil every 10 m. Since spring 2001, continuous frequency domain (FDR) measurements are sampled every 10 min at depths of 15, 30, 45, and 75 cm (CS615, Campbell, USA), over six profiles under a variety of vegetation conditions near the mast. Two campaigns comparing the two-reflectometry systems showed negligible differences.

Soil CO_2 efflux measurements

The soil CO_2 efflux is determined using a portable, closed-chamber system (CIRAS, PP Systems, UK) over a fixed array of soil collars. Thirty cylindrical collars (150 mm high with 100 mm diameter) were located in random positions within a $(50\,m)^2$ area near the mast. We modified the SRC-1 ventilated chamber, introducing a 1-mm (diameter) pressure equilibration tube that communicates with the exterior. A power-bleeding resistor reduces the fan speed by 73% according to recommendations from Le Dantec *et al*. (1999). Soil temperature is measured at a depth of 10 cm adjacent to each collar during measurement. Measurement campaigns were conducted three times in summer 2000, and then roughly monthly from April to December 2001, always during daytime.

Micrometeorological calculations on raw data

The eddy covariance technique measures atmospheric fluxes determined by exchange with an underlying ecosystem (Dabberdt *et al*., 1993). The turbulent-scale covariance between surface-normal (vertical) winds and the relevant scalar (CO_2, H_2O, temperature), measured near the surface, is interpreted as an atmospheric flux representing surface exchange. Long-term applications impose strict conditions on instrumentation and ecosystem and atmospheric conditions. Rarely are all of these conditions satisfied. With no 'true' flux against which to compare, it is difficult to evaluate uncertainties associated with the method. Therefore, eddy fluxes are corroborated via additional flux measurements, surface energy budget closure, and modeling of biological processes that drive the flux. Raw, 20 Hz data were also checked by a quality control program that identified variables (u, v, w, T_v, CO_2, H_2O) that failed statistical criteria over half-hour periods (Vickers & Mahrt, 1997).

Considerable effort has gone towards defining eddy covariance methodologies for determining NEE (Aubinet *et al*., 2000), and yet uncertainty and divergence persists among investigators. When partitioning temporal and spatial scales, 'turbulent' motions may be defined according to different techniques. The co-ordinate system (usually rotated) is also variously defined. Finally, air sampling via an aspirated tube has systematic delay, which must be removed when computing the covariance from instantaneous winds measured by a sonic anemometer.

In this study, the post-processing software EDIRE (University of Edinburgh) was used to treat raw data and compute fluxes, following several different methodologies. Fluxes were computed using three different techniques for high-pass filtering to define turbulence: mean removal, filtering to approximate the removal of a running mean (McMillen, 1988), and linear de-trending (Rannik & Vesala, 1999). A comparison of these techniques is described in the results. Since the study site is exceptionally flat, the computed fluxes are quite insensitive to the exact co-ordinate rotation scheme (analyses not presented here); for consistency within CARBOEUROPE (Aubinet *et al*., 2000) and inter-comparability with results from a nearby mature pine forest (Berbigier *et al*., 2001), half-hour co-ordinate systems were determined by three rotations that orientated the mean wind in the u-direction and maximized the momentum stress in the u–w direction (McMillen, 1988), and fluxes computed using detrending are presented throughout this paper.

Gas sampling by the IRGA was synchronized with the sonic anemometer by correcting for the tube delay, via two different techniques. A fixed system lag was determined by covariance optimization during periods of high flux (afternoon), depending on the presence of the coalescing filter. Alternatively, the lag was determined during each half-hour by covariance optimization over a two-second window enveloping the determined fixed lag, a practice typically employed in on-line flux computations (Moncrieff *et al*., 1997). Optimization over a two-second window was also applied to calculation of the heat flux, where temperature and wind measurements have a known (zero) lag, to identify errors introduced by covariance optimization. One year of data were used in the comparison study.

Measured fluxes were corrected for the loss of high frequency fluctuations in closed-path system (tube), following recommendations from the EUROFLUX methodology (Aubinet *et al*., 2000). Similarity of measured co-spectra between vertical winds and scalars (temperature, CO_2, and H_2O) defined a band-pass frequency range excluding both system-attenuated high frequencies and low frequencies associated with non-stationarity. Co-spectra were normalized according to the covariance integrated over this band-pass range, and averaged over periods with similar wind speed and stability. The ratio of normalized co-spectra for the affected scalar (e.g. CO_2, H_2O) to that for temperature, determined a frequency-dependent transfer function, found to be consistent over periods where the system did not change (i.e. before and after installation of tube heating). Correction factors for CO_2 and H_2O fluxes were determined from the ratio of integrated, normalized co-spectra, using temperature as a reference. The correction factor (C) is larger for H_2O than for CO_2, and depends on the mean wind speed ($\bar{u}$; Moncrieff *et al*., 1997), according to:

$$C = a + b\bar{u} \quad (1)$$

Heating of the sample tube improved the system response, compared to the use of the coalescing filter (Table 2).

Net ecosystem exchange (NEE) of CO_2 was determined directly from (frequency-response-corrected) eddy flux estimates. For airflow, the clear-cut resembles a crop more than a forest, and canopy CO_2 storage likely can be neglected (Baldocchi *et al*., 2001). This assumption is supported by the results of Suyker & Verma (2001), who measured CO_2 profiles over a prairie and found that the storage term contributed very little to the estimate of NEE. Nevertheless, for the purposes of annual integration and determining relationships between nighttime respiration and temperature, only periods with sufficient turbulent mixing were included via the application of a threshold in u^* (Aubinet *et al*., 2000). Isothermal (within small temperature ranges), nocturnal carbon fluxes increased with increasing u^* up to a threshold at $0.5\,m\,s^{-1}$, above which they were invariant with u^*. Micrometeorological fluxes were not corrected to force energy budget closure, an approach used elsewhere (Eugster & Siegrist, 2000).

The flux source area model (FSAM) of Schmid (1994) estimated the flux 'footprints' as the origins of surface exchange. From the friction velocity (u^*) and mean wind speed ($\bar{u}$), we determined the roughness length (z_0) of the ecosystem to be ca. 10 cm. No zero-plane displacement was assumed for the clear-cut ecosystem. The Obukhov length (L) was computed from mean temperature and heat and momentum fluxes, and the standard deviation of the crosswind velocity component (σ_v) was also computed. The ratios of measurement height (z) to z_0 and L, and of σ_v to u^* were input to the model, which was run automatically on data from June 2000 to January 2001 via a computer script, and model recorded outputs included the stream-wise distances to the point of maximum flux contribution (x_{max}) and the furthest contour for 90% flux contribution (e_{90}), describing the surface of flux origin.

Table 2 Frequency response correction parameters (Eqn 1) for two system configurations, with and without the coalescing filter

	Carbon dioxide		Water vapour	
System configuration	*a*	*b*	*a*	*b*
Coalescing filter	1.088	0.0407	1.220	0.1130
Heated intake tube	1.043	0.0432	1.128	0.0695

Empirical models

Non-linear, empirical models of ecophysiological processes were fit by two independent, least-squares methods. The modified Gauss–Newton method (SAS, The SAS Institute Inc., USA) verified the modified Levenberg–Marquardt method (PV-WAVE, Visual Numerics Inc., USA) and yielded estimates of standard error and confidence intervals on model parameters. Standard errors for the empirical parameters were used to generate Monte Carlo simulations with normal distributions ($N = 1000$); uncertainties on annual estimates from the empirical models were determined as the standard deviations from Monte Carlo runs.

Daytime NEE (F_c) measurements were subjected to a further criterion of non-precipitating conditions, grouped by week, and fitted to a hyperbolic dependence on light (PPFD) according to

$$F_c = \frac{a_1 \mathrm{PPFD}}{a_2 + \mathrm{PPFD}} + R_D \quad (2)$$

with fitted parameters a_1, and a_2 and R_D. This formulation has the advantage that the parameters are readily interpreted in ecophysiological terms. The value of F_c at no light (PPFD = 0) is estimated directly as R_D, and may be interpreted as the weekly mean of daytime respiration. The maximum photosynthetic uptake is estimated as a_1 (negative), and the light level (PPFD) corresponding to half the maximum photosynthesis rate as a_2. Furthermore, the ratio a_1/a_2 defines the initial slope of the light response or apparent ecosystem quantum yield (Suyker & Verma, 2001), the sum $a_1 + R_D$ predicts NEE at light saturation, and gross photosynthetic production (GPP) is defined as the difference $R_D - \mathrm{NEE}$. For continuity in modeling ecophysiological processes, five weeks with no reliable model (due to missing data) borrowed regression parameters from adjacent weeks.

Ecosystem respiration estimates were similarly stratified for non-precipitating conditions and sufficient turbulent mixing ($u^* > 0.5\,\mathrm{m\,s^{-1}}$), and fit to an exponential function of temperature (Arrhenius relationship). The soil temperature (T_s, at 5 cm depth) gave the best fit for eddy covariance respiratory fluxes, reflecting the dominance of edaphic processes on respiration. The equation for the resulting respiratory flux of CO_2 (also expressed as F_c) has the form

$$F_c = F_{c,15} \quad Q_{10}^{(T_s - 15)/10} \quad (3)$$

where $F_{c,15}$ is the respiratory flux predicted at a reference temperature ($T_s = 15\,^{\circ}\mathrm{C}$) and Q_{10} describes the sensitivity to temperature; these parameters facilitate comparison with other sites and climates. Because nocturnal eddy covariance fluxes do not always properly estimate surface exchange (e.g. Falge *et al*., 2001a), two respiration estimates were considered. Nighttime eddy covariance fluxes were related to soil temperature, and the daytime, weekly estimate (R_D from Eqn 2) was fit against weekly mean, daytime soil temperature. The soil CO_2 efflux was fit to a function of soil temperature, using spatial averages (over all collars) of the measured flux and adjacent soil temperature for each measurement campaign.

Gap-filling for long-term integration of fluxes

Missing data were filled for annual integration and to provide a continuous database for potential users (e.g. modeling). Data gaps of 2 h or less were filled by direct interpolation. Longer gaps were estimated using the 14-day mean diurnal variation (MDV) method in the case of meteorological data, and semi-empirical methods for missing fluxes (Falge *et al*., 2001a, b). The models described in the Empirical models section estimated CO_2 fluxes, relying on Eqn (2) for daytime and Eqn (3) at night. The heat flux gaps were filled according to monthly linear regressions with net radiation (day), and directly as R_n (night). Missing latent heat flux data were then filled so as to reproduce the typical (lack of) energy budget closure of 87% (day, see below), and estimated as zero (night). Daily precipitation data from a nearby (8 km) meteorological station were used to fill a summer gap in pluviometry.

Results

In this paper, all data are presented on universal time (UTC), which leads local solar time by 7 min. Figure 1 presents a summary of meteorological conditions over the study period. The year 2000 was relatively warm with an extremely wet autumn. The following winter and spring were likewise mild, but rather dry. While the summer began warm and dry, July and August were relatively wet and cool, with no evidence of drought stress in Les Landes. Autumn 2001 was initially mild and dry, but November was cold and dry, and the year finished with several weeks below freezing, relatively rare for the region.

Over this period, data coverage for eddy fluxes of CO_2 and latent heat is 86%, and slightly better for the heat flux. Several entire weeks are missing due to pump and software failures, and the system was down for one hour per week during maintenance and data collection. Table 3 summarizes measurements rejected by quality control program.

The footprint analysis suggests that measured turbulent fluxes originated from the ecosystem. The Schmid (1994) model provided footprint estimates for 95% of daytime data for which it was run (slightly less in winter); model runs that gave errors were ignored. The distance to maximum contribution (x_{max}) was always within the ecosystem in summer, and 95% in winter. The 90% flux contribution contour (e_{90}) fell within the ecosystem 80% of the time in summer, and 20% in winter. At night, both the model and footprints were less well behaved. The model ran successfully only 30% of the time, and determined that x_{max} was within the ecosystem about 80% of the time (seasonally invariable), or 100% when the u^* threshold was applied. Only 10–20% of the successful nighttime model runs determined that e_{90} was within the ecosystem.

Methodological comparisons

While three different flux calculation techniques (mean removal, filtering, and de-trending) yield negligible differences, ecosystem exchange is quite sensitive to the

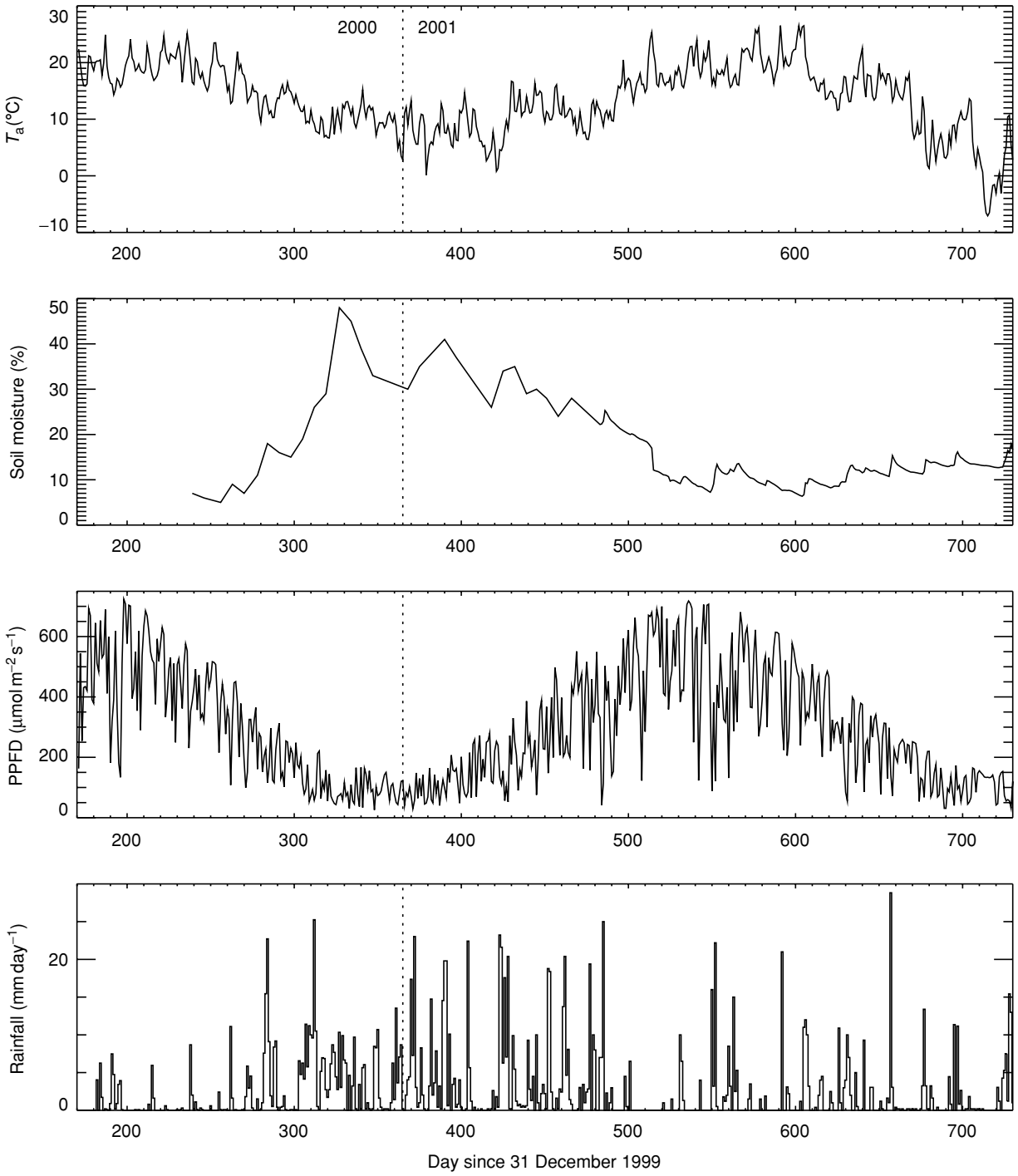

Fig. 1 Meteorological conditions in the clear-cut during the study period: daily means of air temperature (T_a), volumetric soil moisture content (%), and photosynthetic photon flux density (PPFD, μmol m^{-2} s^{-1}), and rainfall (mm day^{-1}).

method used to determine the system lag. For the CO_2 flux, time lags optimized every half-hour result in about 5% more flux at night (averaged over several months of comparison), but no difference in the day, relative to the fixed lag covariance. Integration of this bias leads to an annual over-estimation of NEE of carbon by 55%. A similar comparison for temperature (certainly not a lagged signal) indicates that optimizing the covariance for each half-hour leads to a 5–10% over-estimation of the nighttime heat flux magnitude, but no difference during

the day. All of the fluxes examined in the analyses that follow were computed using a fixed lag.

Carbon fluxes

Diurnal trends in NEE for the clear-cut follow patterns that are familiar from forest ecosystems, but with smaller amplitude. Figure 2 shows the mean diurnal NEE for 4 months, representing the seasons. At solar noon (very nearly 12:00 GMT), photosynthetic activity is always at least large enough to balance respiration in the monthly mean. Thus on fair, sunny afternoons the ecosystem consistently fixes carbon. Daytime uptake typically peaks near 4 $\mu mol\,m^{-2}\,s^{-1}$ in the summer, is about half that in the fall and spring, and is near zero in winter. However, integrated over an average day, total ecosystem respiration is larger than photosynthetic fixation during every month.

The dependence of photosynthesis on light is evident in the form of weekly light response curves; Fig. 3(a–d) presents 4 weeks representative of the seasons. At all times of the year, upwards fluxes dominate at low light levels, but give way to increasingly downward fluxes with increasing light until the trend levels off (i.e. the response to light forcing saturates) above ca. 1000 $\mu mol\,m^{-2}\,s^{-1}$. The magnitudes of NEE, radiation, and temperature are all highest during the summer (Fig. 3a), moderate in the spring (Fig. 3d) and autumn (Fig. 3b), and smallest in winter (Fig. 3c). The regression models are not over-parameterized, always yielding non-zero parameters. Table 4 presents the regression parameters associated with each of the models drawn in Fig. 3.

Table 3 Percentage of half-hours (%), by variable and year, flagged and rejected by the quality control package

	u	v	w	T_v	CO_2	H_2O
2000	0.2	0.4	0.3	0.7	4.5	3.2
2001	0.5	0.3	0.3	0.9	1.8	1.1

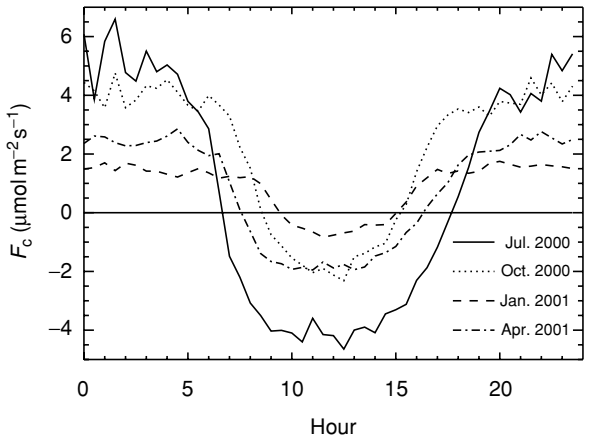

Fig. 2 Diurnal trends in NEE of carbon (F_c, $\mu mol\,m^{-2}\,s^{-1}$), loss from the clear-cut for 4 months representing the seasons.

The weekly empirical parameters follow seasonal trends corresponding to temperature and phenology. Figure 4 shows the parameters a_1 (GPP at light saturation) and R_D (daytime ecosystem respiration) over the course of the study period; for the sake of comparison, soil respiration measurements are also plotted. Respiration is highest in the hottest part of summer, except during periods of very dry soil (September 2001), and photosynthetic capacity is also greatest during the period of maximum leaf area for the dominant summer species (grasses). While seasonal variations in a_1 and R_D are clearly correlated, the within-week, asymptotic correlation between the two parameters is very small. It is worth noting that R_D appears to lag a_1 by a week or two during the spring and summer, but this is not observed for late summer and autumn. The parameter a_2, describing the curvature of the parabolic model, shows no clear seasonal trend.

Respiration, the dominant process determining the clear-cut carbon fluxes, is estimated via several techniques and related to soil temperature according to Eqn (3). The eddy flux from nighttime periods satisfying the u^* criterion is related to the soil temperature at 5 cm depth (Fig. 5). The parameters $F_{c,15}$ and Q_{10} from the Arrhenius equation (Table 5) show significant respiration with a somewhat weak temperature dependence. To avoid uncertainties associated with nighttime eddy covariance, the temperature dependence of daytime respiration (empirical parameter R_D) also is considered as a function of the relevant soil temperature (Fig. 6). The results are similar to the nighttime flux analysis, but estimated daytime respiration is somewhat weaker, and with a weaker temperature dependence than at night. Finally, soil respiration determined from chamber measurements (Fig. 7) is consistent with the ecosystem respiration estimates. Temperature-independent soil respiration is a major fraction of total respiration (ratio of $F_{c,15}$ values), with the suggestion of a slightly higher dependence on soil temperature (Q_{10}), but no statistical difference.

Although the clear-cut ecosystem is capable of fixing carbon during fine weather, it is a consistent source of atmospheric CO_2. Figure 8 shows the mean daily release of CO_2 from the ecosystem and the accumulated carbon loss over the study period. During summer, at peak respiratory and photosynthetic rates, dramatic changes can be seen from day to day. The ecosystem fixes carbon during sunny periods, but respiration overshadows light-limited photosynthesis. In the annual balance,

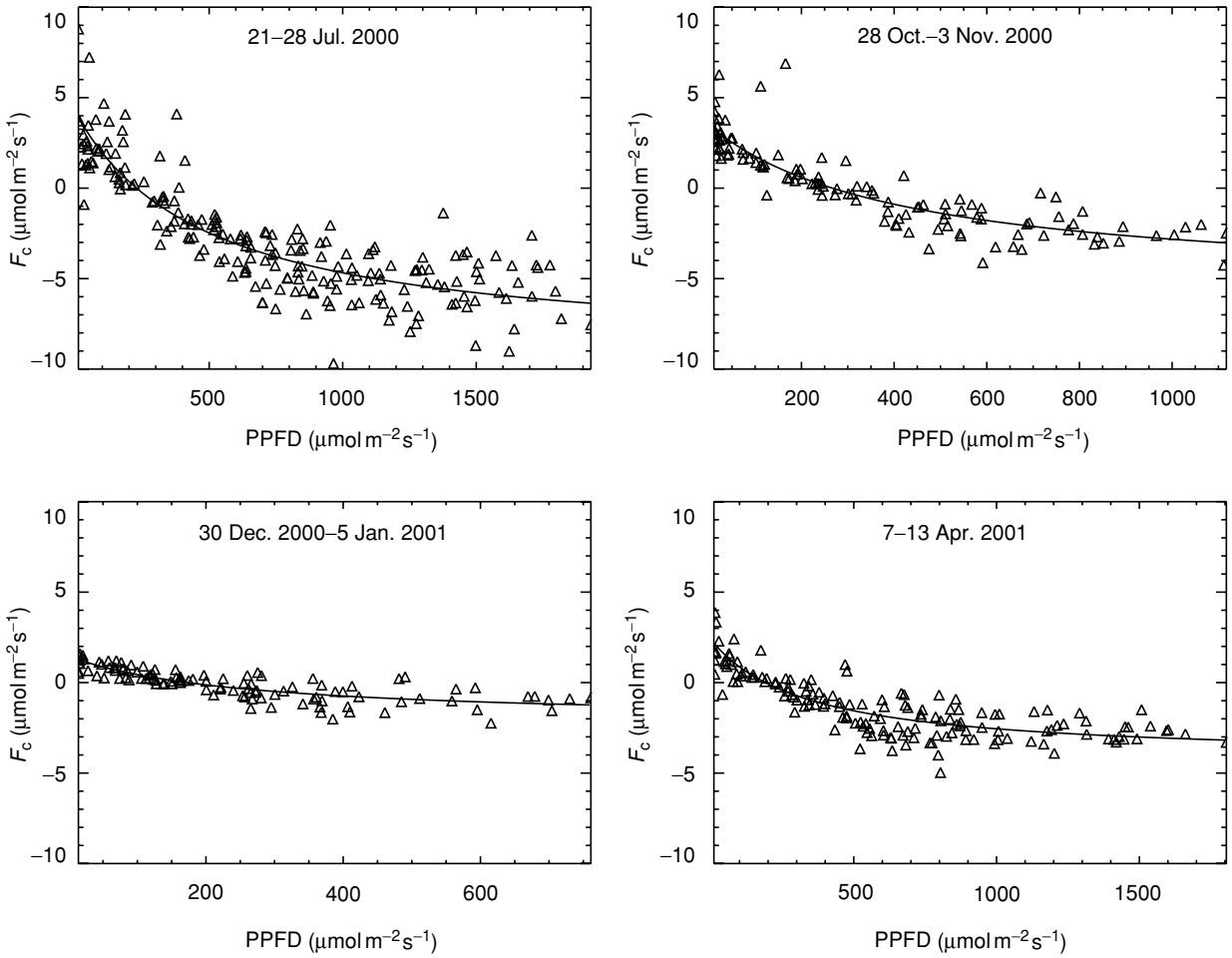

Fig. 3 Light response curves; NEE of carbon (F_c, μmol m^{-2} s^{-1}) vs PPFD (μmol m^{-2} s^{-1}) for selected weeks corresponding to the months presented in Fig. 2. Empirical model parameters R_D, a_1, and a_2 (defined in Eqn 2) are also given.

Table 4 Non-linear regression parameters, estimated standard error, and 95% confidence intervals for the 4 weeks, presented in Fig. 3, and representative of the four seasons

Parameter	Fig. 3	Season	Estimate	SE	Lower 95%	Upper 95%
R_D	A	Summer	4.17	0.65	2.90	5.45
	B	Fall	3.48	0.22	3.04	3.93
	C	Winter	1.45	0.18	1.11	1.81
	D	Spring	2.36	0.24	1.88	2.86
a_1	A	Summer	−13.2	0.60	−14.4	−12.0
	B	Fall	−8.94	0.71	−9.68	−6.84
	C	Winter	−3.59	0.34	−4.26	−2.92
	D	Spring	−6.59	0.27	−7.12	−6.06
a_2	A	Summer	496	69.6	358	633
	B	Fall	418	95.1	230	606
	C	Winter	253	84.7	85.6	421
	D	Spring	339	53.7	233	444

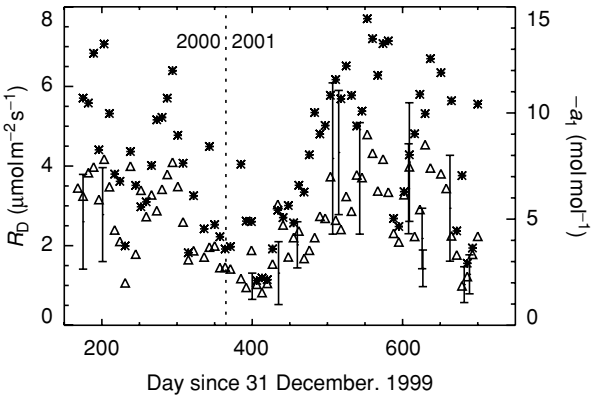

Fig. 4 Seasonal variation in weekly empirical model parameters for the light-response curves (Eqn 2), and soil respiration. Estimated daytime respiration (R_D, μmol m^{-2} s^{-1}, triangles), soil respiration (brackets showing mean, and SEM), and maximum photosynthetic capacity ($-a_1$, mol mol^{-1}, asterisks) are plotted vs time.

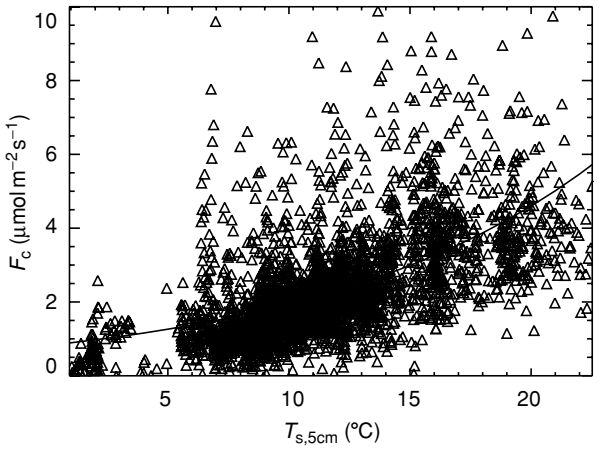

Fig. 5 NEE of carbon (F_c, μmol m^{-2} s^{-1}) for nocturnal periods with sufficient turbulent mixing ($u^* > 0.5$ m s^{-1}) as a function of soil temperature (T_s). Empirical model parameters $F_{c,15}$ and Q_{10} (defined in Eqn 2) are also given. $N = 3472$.

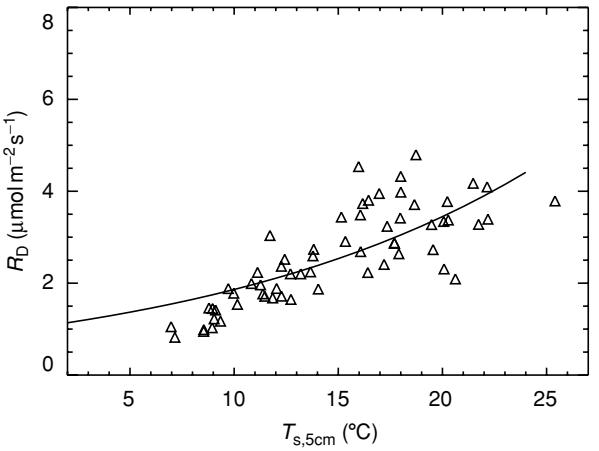

Fig. 6 Daytime respiration (R_D, μmol m^{-2} s^{-1}) from weekly empirical models as a function of weekly mean, daytime soil temperature (T_s). Empirical model parameters $F_{c,15}$ and Q_{10} (defined in Eqn 2) are also given. $N = 63$.

Table 5 Parameters for the Arrhenius equation by respiration component. Standard errors and 95% confidence intervals (lower and upper) are included for each parameter

Respiratory flux component	Estimate	SE	95% confidence intervals	
			Lower	Upper
$F_{c,15}$				
NEE night (Fig. 5)	2.99	0.03	2.92	3.05
R_D day (Fig. 6)	2.53	0.10	2.34	2.72
F_c Soil (Fig. 7)	2.60	0.19	2.18	3.01
Q_{10}				
NEE night (Fig. 5)	2.37	0.06	2.25	2.49
R_D day (Fig. 6)	1.85	0.13	1.59	2.12
F_c soil (Fig. 7)	2.64	0.60	1.35	3.93

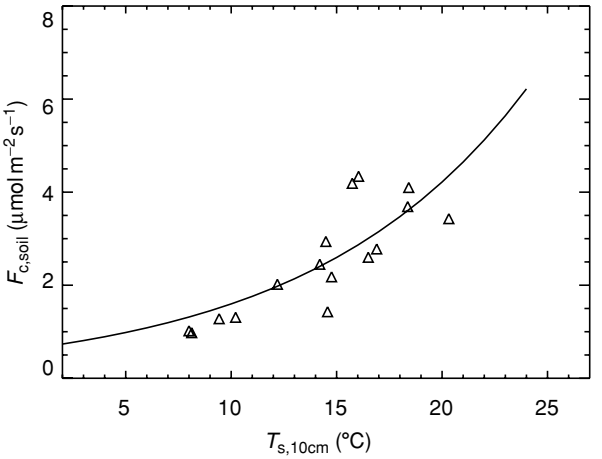

Fig. 7 Soil respiration ($F_{c,soil}$, μmol m^{-2} s^{-1}) from chamber measurement campaigns as a function of soil temperature. Empirical model parameters $F_{c,15}$ and Q_{10} (defined in Eqn 2) are also given. $N = 16$, where each point is the average over all soil collars.

decomposition of organic matter accumulated by the forest prior to cutting clearly dominates photosynthetic regeneration of the ecosystem.

Integrated carbon loss over the study period approaches 400 g m^{-2} (Fig. 8). The estimated annual balance depends on the 365 days chosen, and shows an anti-correlation with annual PAR (Fig. 9). When considering the first year of measurements (June–June), the annual carbon loss is ca. 200 g m^{-2}. However, the ecosystem lost less carbon during the sunny summer of 2000 (relative to 2001). Then, beginning in autumn (around day 635), the year 2000 became very cloudy and rainy, while 2001 was sunnier and showed less carbon loss. Finally, December 2001 was sunny but very cold, with temperatures below zero day and night for much of the month; however, this extreme temperature event does not appear to have changed NEE very much relative to 2000. Total carbon loss during 2001 was 290 g m^{-2}. These results are quite sensitive to the application of the u^* criterion, which rejected about two thirds of the nighttime data. If this criterion is not applied, the anti-correlation with annual PAR disappears, and annual carbon loss decreases by 50%.

The empirical models partition NEE into respiratory and photosynthetic components, allowing annual estimation of GPP, total ecosystem respiration (TER) and the soil efflux. Integration of GPP relied on PPFD measurements and weekly parameters (a_1 and a_2). Respiration was modeled via the Arrhenius equation, with the

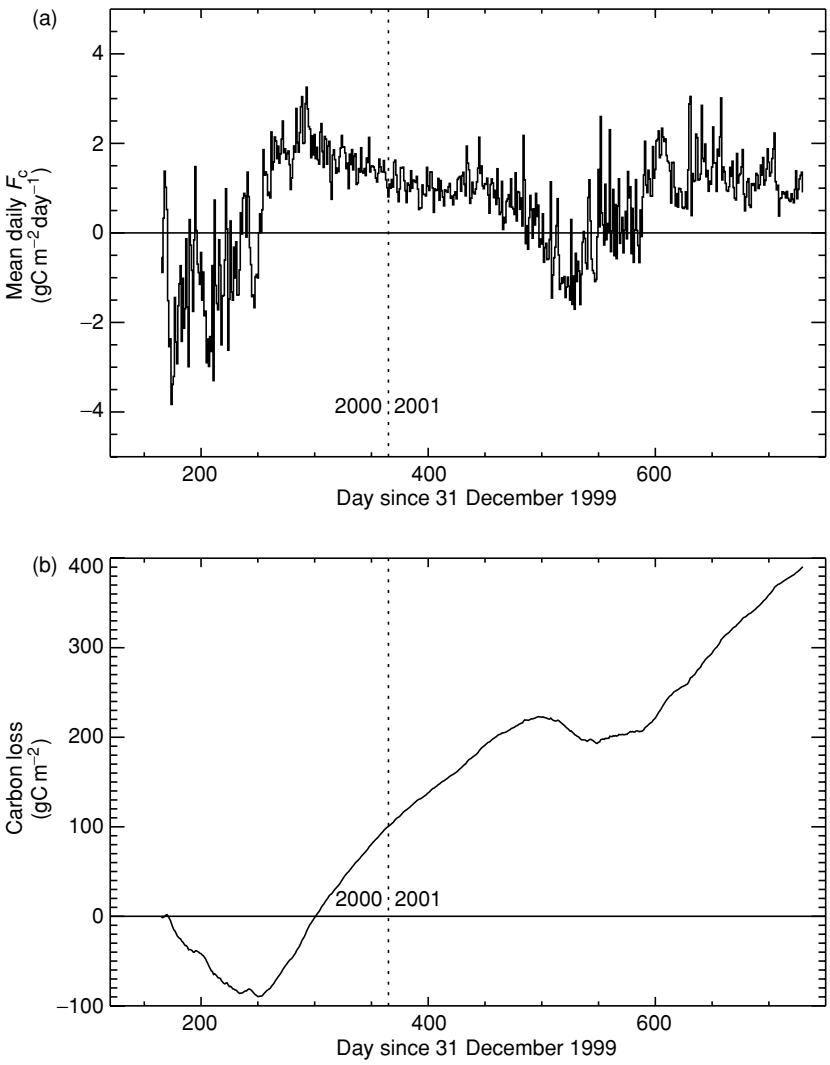

Fig. 8 Time trends in carbon loss from the clear-cut over the study period: (a) daily carbon loss (F_c, gC m^{-2} day^{-1}) and (b) accumulated carbon loss (gC m^{-2}).

appropriate temperature and parameters: nighttime TER via eddy flux results (Table 5; Fig. 5); daytime respiration via mean, daytime, weekly soil temperature (Table 5; Fig. 6), yielding agreement with direct estimates from R_D; and soil respiration via soil temperature (Table 5; Fig. 7). For the calendar year 2001, which had 9227 mol m^{-2} of available photosynthetic photons and a mean soil temperature of 13.6 °C, we estimated 727 ± 150 gC m^{-2} of GPP and 996 ± 10 gC m^{-2} of TER, where about 93% of respiration originated below ground (927 ± 69 gC m^{-2} of annual soil efflux).

Other fluxes and relationships

The lack of energy balance closure for the clear-cut is consistent with other eddy covariance studies. A typical period of high fluxes (i.e. summer) and minimal gaps was chosen to display this. Figure 10 shows that the turbulent fluxes of latent and sensible heat explain about 87% of energy available to the atmosphere at the surface, from net radiation and the soil heat flux (G). The daytime energy budget closure is very similar to that shown in Fig. 10, while nighttime energy budget closure is problematic, application of the u^* criterion notwithstanding.

Figure 11 shows the seasonal trends in the sensible and latent heat fluxes from the ecosystem, demonstrating that more energy typically goes into sensible heat loss than to evapotranspiration (Bowen ratio exceeding unity). The annual sums for the 2001 calendar year were 928 MJ m^{-2} of sensible heat and 895 MJ m^{-2} of latent heat (equivalent to 358 mm of evapotranspiration), vs 1956 MJ m^{-2} of net radiation. Annual integration of the soil heat flux was not possible, but assuming that the annual sum is negligible, the annual gap in the energy budget is of order 133 MJ m^{-2} or 7% of available energy. Annual precipitation for 2001 was 875 mm.

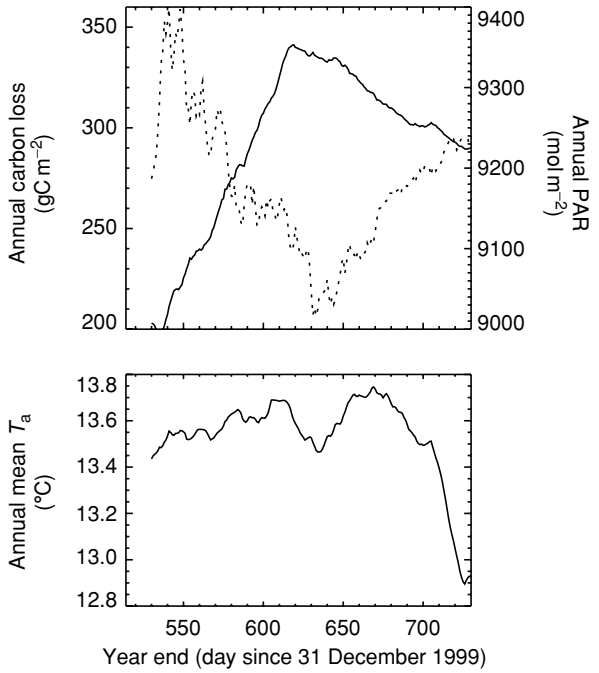

Fig. 9 Annual running means of (a) net carbon flux (gC m^{-2}), incoming PPFD (mol m^{-2}), and (b) temperature as a function of the date of the end of the year. To facilitate comparison with Fig. 1, the final day of the annual integration is plotted on the *x*-axis as the day since 31 December 1999.

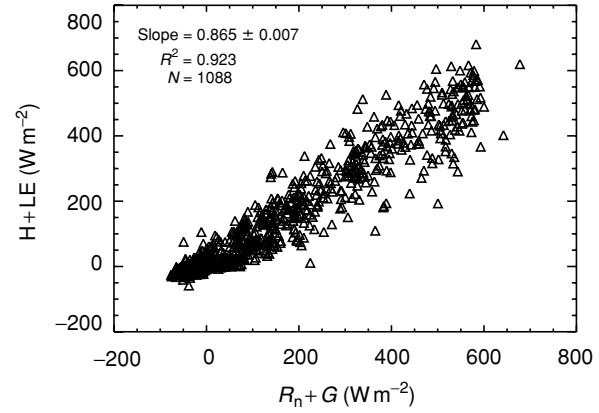

Fig. 10 The energy balance for the month of May 2001: the sum of turbulent sensible and latent heat fluxes (H + LE, W m^{-2}) are plotted against energy available from radiative and soil heat fluxes ($R_n + G$, W m^{-2}).

Discussion

Despite significant GPP, and inter-annual variability manifest in just 18 months of measurements, the clear cut is clearly an annual source. A comparison of flux-computation methodologies has revealed some uncertainty concerning the means of determining the system lag. Nevertheless, a combination of empirical modeling, independent soil CO_2 efflux measurements, a footprint model, and surface energy budget closure lends credibility to the statement that the clear-cut loses approximately 300 gC m^{-2} annually. Some of the major sources of uncertainty are now discussed.

Both the increasing speed and disk space of microcomputers, and the availability of tools such as the (free) EDIRE software, allow the application of an array of methodologies to determine eddy covariance fluxes and bound their uncertainties. For a flat, and relatively homogeneous site such as the Bilos clear-cut, the means of isolating and defining turbulent motions (in the temporal domain via averaging, filtering, and de-trending) appears to be of little consequence. This is encouraging considering the divergence of methodologies applied used at different sites (see Micrometeorological calculations on raw data section). In contrast, the computed flux is sensitive to the correct lag time for the closed-path system. Covariance optimization techniques were designed as part of on-line flux computation, developed due to limitations on computer speed and disk space. Our analyses showed that this issue requires somewhat more attention, as covariance optimization appears to overestimate the nighttime flux from the clear-cut by 5% or more. Such a selective systematic error, affecting nighttime only, leads to large errors in the estimation of annual fluxes (Moncrieff *et al*., 1996), amounting to 55% over-estimation according to our calculations. We recommend that fluxes be computed via post-processing, and analyses of Bilos data suggest that the system lags are best applied on a systematic basis.

The *u** threshold (0.5 m s^{-1}) is similar to those typically applied over forest (e.g. Lindroth *et al*., 1998; Aubinet *et al*., 2001; Berbigier *et al*., 2001), but high compared to that used in an experiment with a similar measurement height over a dynamically similar surface (0.2 m s^{-1}, Suyker & Verma, 2001). This may reflect the physical dimensions of the ecosystem: relative to nearby mature stands, the clear-cut is a sheltered depression, possibly de-coupled from the main flow aloft on stable nights. Such a situation favors the development of non-turbulent, nocturnal features such as gravity waves, which also would contribute to uncertainties determining the system lag during periods of weak winds and little turbulence.

The techniques applied here to corroborate the eddy flux data point to greater uncertainty in the nighttime flux, relative to day. Both surface energy budget closure and footprint models suggest likely problems with the nighttime fluxes. Soil CO_2 effluxes were measured only during the day. However, while the uncertainty in any half-hour flux estimate might be high at night, we have found no evidence of systematic errors in nighttime fluxes, once selected according to the *u** threshold.

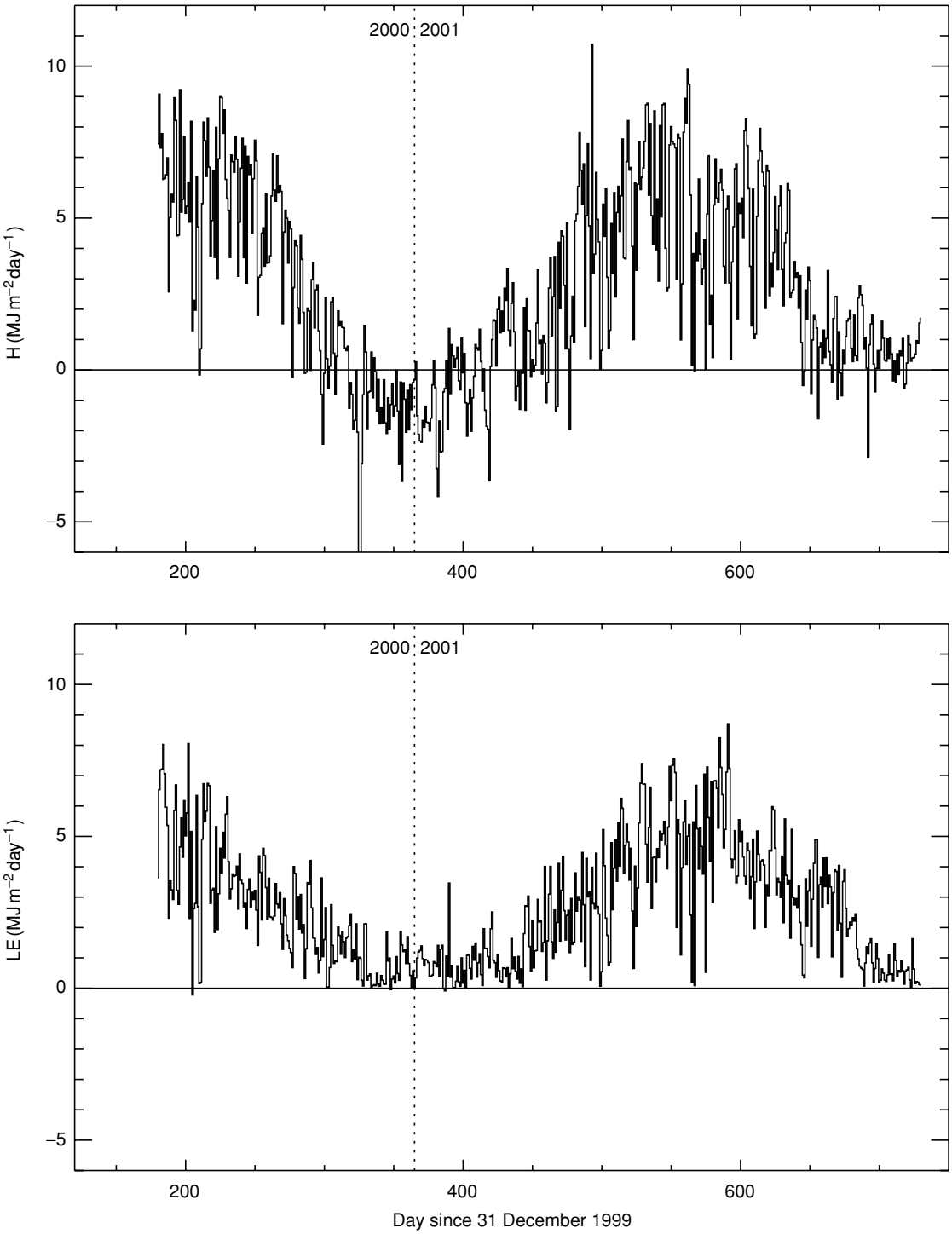

Fig. 11 Time trends in sensible (H) and latent (LE) heat loss (MJ m^{-2} day^{-1}) from the clear-cut over the study period.

We have found weekly empirical modeling of eddy fluxes a powerful tool for numerous uses of the data. The developed models were essential for gap-filling and hence annual integration. Seasonal trends in the photosynthetic parameter a_1, independent of available light, give some insight into the photosynthetic capacity and phenology of the species populating the clear-cut. Furthermore, the observation that respiration (R_D) lags photosynthesis (a_1) during periods of high productivity (mid summer 2000 and spring 2001) may reflect the

physiological dependence of soil respiration on the availability of photosynthetic assimilates, shown elegantly by girdling experiments on Scots Pine stands (Hogberg *et al*., 2001); this point will deserve further attention in future studies. The empirical models were also important for decomposing directly measured NEE into GPP and TER components, and enabling comparison with soil efflux measurements. Respiration components estimated by various techniques showed consistent behavior, with similar $F_{c,15}$ and Q_{10} values derived in every case. This lends credence to the individual estimates, and suggests that the soil is the dominant respiring component of the clear-cut ecosystem. The NEE determined from the models (as TER-GPP) is the same as that determined from integration of eddy fluxes, within the uncertainty in the model estimate.

Various investigators have estimated uncertainties in eddy covariance annual NEE at 10–20% (e.g. Goulden *et al*., 1996; Anthoni *et al*., 1999; Aubinet *et al*., 2001), and energy budget considerations lead to similar conclusions about uncertainties in the estimate of turbulent exchange at the Bilos clear-cut. Since ecosystem/fetch size is a concern when estimating nighttime respiration from the clear-cut, we derived a different TER estimate by determining empirical model parameters only from fluxes with footprints modeled as within the ecosystem; this estimate had greater uncertainty owing to high data rejection, and led to a 15% decrease in the estimate of annual TER. We interpret this as representing additional uncertainty regarding nighttime processes, but not necessarily as a better estimate of TER for the clear-cut. Both modeling and integration of direct measurements suggests that the Bilos clear-cut is an annual carbon source of 290 $gC\,m^{-2}$, to within ca. 25%.

Probably due to 2000 and 2001 climatic extremes, a certain degree of inter-annual variability is manifest in the analysis of just 18 months of data. The variation in annual NEE according to the selected 365-day period corresponds to large differences in available sunlight. Carbon release by the clear-cut was enhanced during cloudy periods (fall of 2000 and summer of 2001) when light limited photosynthesis. However, a prolonged cold spell in December of 2001 does not appear to have affected NEE, possibly because both photosynthesis and respiration suffered from the sub-zero temperatures. Of course, when interpreting these results it should be remembered that evolution of the recovering ecosystem might also yield annual differences, independent of the weather. Clearly, continued measurements are needed to elucidate relationships between annual NEE and climate.

The lack of energy balance closure is similar to those reported at other sites devoted to annual NEE measurements; no consensus has yet been reached to explain this lack of closure. The Bowen ratio is typically unity or slightly larger during the growing season, and a bit higher towards the end of the (dry) summer; this is larger than that reported for forest sites, and consistent with the decrease in photosynthetic activity. Finally the discrepancy between precipitation and evapotranspiration (of order 500 $mm\,a^{-1}$) for the clear-cut is large compared with drainage estimates for Les Landes forest (290 $mm\,a^{-1}$, CEMAGREF, unpublished data 2002), which ought to be expected when comparing a clear-cut with evapotranspiring forest stands.

As a beginning toward understanding the effect of clear-cutting on a forest-atmosphere exchange, we consider fluxes from the clear-cut vs those from a mature maritime pine stand in Les Landes. Table 6 shows the 2001 annual fluxes from Bilos and several years' data from the mature 'Bray' stand 30 km to the NE. The 1997–1998 Bray site estimates represent the undisturbed forest at age 28 (Berbigier *et al*., 2001). Data simultaneous to those from clear-cut are also presented (2001); however, these data may include the effects of disturbance introduced by the December 1999 windstorm, which felled swathes of trees at the Bray site. The periods compared have similar annual mean PPFD; however, 2001 was somewhat dry, and 1997 particularly warm, relative to climatic norms.

The greatest difference is in the annual carbon budget; while the mature site is a sink, the clear-cut is an annual source. The recovering clear-cut has about one-third the GPP of the forest, where understorey contributions have been estimated at 15% (Delzon *et al*., in preparation). Although rich in accumulated soil carbon and harvest residues, the clear-cut respires only two-thirds as much

Table 6 Comparison of annual ecosystem fluxes from the clear-cut (Bilos) in 2001 and those reported for a mature forest (Bray) at age 28 in 1997–1998 (Berbigier *et al*., 2001) and at age 31 in 2001 (Berbigier, unpublished data), both in Les Landes

Annual exchange	Bilos (age = 0)	Bray (age = 28)	Bray (age = 31)
NEE carbon ($gC\,m^{-2}$)	290	−575	−498
GPP ($gC\,m^{-2}$)	727	2255	2025
TER ($gC\,m^{-2}$)	996	1680*	1527
PPFD ($mol\,m^{-2}$)	9227	9296	9308
R_n ($MJ\,m^{-2}$)	1956	3006	2746
T_{air} (°C)	13.2	15.0*	13.4
H ($MJ\,m^{-2}$)	928	620	515
LE ($MJ\,m^{-2}$)	895	1592	1491
Evaporation (mm)	358	666	624
Precipitation (mm)	875	930	515†

*Respiration (TER) and temperature from the Bray site are for the period March 1997–February 1998.
†This figure lacks 5 months of precipitation measurements.

as the forest annually; this may depend on the warmer year considered for the Bray site, but it lends credence to the hypothesis that respiration depends on carbon allocation from recent photosynthetic activity by living biomass (Janssens *et al*., 2001).

Although incident sunshine (PPFD) is very similar, the two ecosystems also show very different partitioning of available energy. In the clear-cut, absorbed solar energy raises the surface temperature, leading to large losses of sensible heat (H) and especially infrared radiation, thus reducing R_n by a third. The forest maintains a cooler surface, using more energy for evapotranspiration. The residual term in the annual energy budget (neglecting soil fluxes) is ca. 7% in Bilos, but more than 20% in the forest, such that further details cannot be extracted from the comparison.

The effects of harvest-disturbance on carbon fluxes at Bilos are mild relative to reports from the literature. Initially, clear-cutting was thought to stimulate decomposition by warming the soil and adding harvest residues (e.g. Ewel *et al*., 1987). However, more recent studies of pine forests have reported marked reductions in soil respiration as a result of clear-cutting. Arneth *et al*. (1998b) found that, increased heterotrophic respiration notwithstanding, the loss of root respiration due to harvesting of New Zealand Monterrey pines reduced total belowground respiration by two thirds. While this case may be extreme due to the destruction of root systems by 'rip-lining' (Arneth *et al*., 1998a), Striegl & Wickland (1998) also estimated that clear-cutting of jack pine reduced soil respiration by 60%. In Bilos, abundant re-growth appears to mitigate disturbance effects on photosynthesis and respiration. Harvest practices leaving the understorey to recover also impact the ecosystem energy balance.

Few studies have examined the effects of clear-cutting on the energy balance. Amiro (2001) measured reductions in net radiation, latent heat, and also sensible heat fluxes due to clear-cutting of aspen forest. In that campaign, mineral soil exposure during mounding (preparation for planting) led to very large fluxes and retention of soil heat, which explains the reduced sensible heat flux. The general expectation that logging would increase heat fluxes and thus the Bowen ratio (Schulze *et al*., 1999) is confirmed from the Bilos–Bray comparison presented here.

Summary and conclusions

From 18 months of closed-path eddy covariance measurements, we have estimated an annual carbon loss of 200–350 $gC\,m^{-2}$ for a clear-cut maritime pine ecosystem in Les Landes (SW France), depending on the 365-day period considered. Soil respiration is the dominant process driving the carbon exchange, but bio-diverse re-growth was already fixing carbon during sunny periods just a few months after clear cutting, and also through winter senescence of the dominant vegetation (grass). Methodological comparisons showed that the correct determination of the system lag for gas sampling is important for accurate estimation of eddy fluxes, particularly at night when lag optimization techniques may be unreliable. Weekly empirical models, based on light and temperature, filled gaps and partitioned the net carbon exchange into photosynthetic and respiratory components.

Comparison with a mature forest showed a marked effect of clear-cutting on both the carbon balance and surface energy partitioning. Both the turbulent fluxes of latent and sensible heat, and also net radiation, are markedly different between the forest and the clear cut. However, these effects appear to be mitigated by harvest practices that allowed rapid re-growth of the understorey. With additional understanding of the evolving budgets of carbon, water, and energy over a forest life cycle, continuing results from the Bilos site will contribute to a long-term goal of sustainable development in the managed forest that is Les Landes.

Acknowledgements

This work was funded by the EC Environment and Climate Research Programme CARBOAGE project (contract ENV4-CT97-0577), with support from the public interest group GIP ECOFOR, and the Aquitaine regional project 'Bilan de Carbone de la Forêt Landaise'. We thank the commune of Salles and the French ONF for support. We also thank the Ecophysiology team of Pierroton for all their support, J. Hearn of VNI (Paris) for help installing software, and H.P. Schmid for free use of his FSAM software. Finally, we thank two anonymous referees for comments that improved the manuscript significantly.

References

Amiro BD (2001) Paired-tower measurements of carbon and energy fluxes following disturbance in the boreal forest. *Global Change Biology*, **7**, 253–268.

Anthoni PM, Law BE, Unsworth MH (1999) Carbon and water exchange of an open-canopied ponderosa pine ecosystem. *Agricultural and Forest Meteorology*, **95**, 151–168.

Arneth A, Kelliher FM, Gower ST *et al.* (1998a) Environmental variables regulating soil carbon efflux following clear-cutting of a *Pinus radiata* D. Don plantation. *Journal of Geophysical Research*, **103**, 5695–5705.

Arneth A, Kelliher FM, McSeveny TM *et al.* (1998b) Assessment of annual carbon exchange in a water-stressed *Pinus radiata* plantation: an analysis based on eddy covariance measurements and an integrated biophysical model. *Global Change Biology*, **5**, 531–545.

Aubinet M, Chermanne B, Vandenhaute M *et al.* (2001) Long term carbon dioxide exchange above a mixed forest in the Belgian Ardennes. *Agricultural and Forest Meteorology*, **108**, 293–315.

Aubinet M, Grelle A, Ibrom A *et al.* (2000) Estimates of the annual net carbon and water exchange of forests: the EUROFLUX methodology. *Advances in Ecological Research*, **30**, 113–173.

Baldocchi D, Falge E, Gu L *et al.* (2001) FLUXNET: a new tool to study the temporal and spatial variability of ecosystem-scale carbon dioxide, water vapor, and energy flux densities. *Bulletin of the American Meteorological Society*, **82**, 2415–2434.

Berbigier P, Bonnefond J-M, Mellmann P (2001) CO_2 and water vapour fluxes for 2 years above Euroflux forest site. *Agricultural and Forest Meteorology*, **108**, 183–197.

Dabberdt WF, Lenschow DH, Horst TW *et al.* (1993) Atmosphere-surface exchange measurements. *Science*, **260**, 1472–1480.

Eugster W, Siegrist F (2000) The influence of nocturnal CO_2 advection on CO_2 flux measurements. *Basic and Applied Ecology*, **1**, 177–188.

Ewel KC, Cropper WP, Gholz HL (1987) Soil CO_2 evolution in Florida slash pine plantations. I. Changes through time. *Canadian Journal of Forest Research*, **17**, 325–329.

Falge E, Baldocchi D, Olson R *et al.* (2001a) Gap filling strategies for defensible annual sums of net ecosystem exchange. *Agricultural and Forest Meteorology*, **107**, 43–69.

Falge E, Baldocchi D, Olson R *et al.* (2001b) Gap filling strategies for long term energy flux data sets. *Agricultural and Forest Meteorology*, **107**, 71–77.

Geider RJ, Duelucia EH, Falkowski PG *et al.* (2002) Primary productivity of planet earth: biological determinants and physical constraints in terrestrial and aquatic habitats. *Global Change Biology*, **7**, 849–882.

Goulden ML, Munger JW, Fan S *et al.* (1996) Measurements of carbon sequestration by long-term eddy covariance: methods and a critical evaluation of accuracy. *Global Change Biology*, **2**, 169–182.

Hogberg P, Nordgren A, Buchmann N *et al.* (2001) Large-scale forest girdling shows that current photosynthesis drives soil respiration. *Nature*, **411**, 789–792.

Janssens IA, Lankreijer H, Matteucci G *et al.* (2001) Productivity overshadows temperature in determining soil and ecosystem respiration across European forests. *Global Change Biology*, **7**, 269–278.

Law BE, Thornton PE, Irvine J *et al.* (2001) Carbon storage and fluxes in ponderosa pine forests at different developmental stages. *Global Change Biology*, **7**, 755–777.

Le Dantec V, Epron D, Dufrêne E (1999) Soil CO_2 efflux in a beech forest: comparison of two closed dynamic systems. *Plant and Soil*, **214**, 125–132.

Lindroth A, Grelle A, Morén A (1998) Long-term measurements of boreal forest carbon balance reveal large temperature sensitivity. *Global Change Biology*, **4**, 443–450.

McMillen RT (1988) An eddy correlation technique with extended applicability to non-simple terrain. *Boundary-Layer Meteorology*, **43**, 231–245.

Moncrieff JB, Malhi Y, Leuning R (1996) The propagation of errors in long-term measurements of land-atmosphere fluxes of carbon and water. *Global Change Biology*, **2**, 231–240.

Moncrieff JB, Massheder JM, de Bruin H *et al.* (1997) A system to measure surface fluxes of momentum, sensible heat, water vapour and carbon dioxide. *Journal of Hydrology*, **188–189**, 589–611.

Porté A (1999) *Modélisation Des Effets Du Bilan Hydrique Su la Production Primaire et la Croissance D'un Couvert de Pin Maritime (Pinus Pinaster Ait) En Lande Humide*. Doctoral, Université de Paris-Sud, 196.

Post WM, Kwon KC (2000) Soil carbon sequestration and land-use change: processes and potential. *Global Change Biology*, **6**, 317–327.

Rannik Ü, Vesala T (1999) Autoregressive filtering versus linear detrending in estimation of fluxes by the eddy covariance method. *Boundary-Layer Meteorology*, **91**, 259–280.

Schmid H-P (1994) Source areas for scalars and scalar fluxes. *Boundary-Layer Meteorology*, **67**, 293–318.

Schulze E-D, Lloyd J, Kelliher FM *et al.* (1999) Productivity of forests in the Eurosiberian boreal region and their potential to act as a carbon sink – a synthesis. *Global Change Biology*, **5**, 705–722.

Striegl RG, Wickland KP (1998) Effects of a clear-cut harvest on soil respiration in a jack pine – lichen woodland. *Canadian Journal of Forest Research*, **28**, 534–539.

Suyker AE, Verma SB (2001) Year-round observations of the net ecosystem exchange of carbon dioxide in a native tallgrass prairie. *Global Change Biology*, **7**, 279–289.

Valentini R, Matteucci G, Dolman AJ *et al.* (2000) Respiration as the main determinant of carbon balance in European forests. *Nature*, **404**, 861–865.

Vickers D, Mahrt L (1997) Quality control and flux sampling problems for tower and aircraft data. *Journal of Atmospheric and Oceanic Technology*, **14**, 512–526.

Appendix

Plant species in the clear-cut, rated with an abundancy index (0–6)

	Woody species			
	>2 m	0.3–2 m	Graminae	Mosses
Pinus pinaster	3	2	1	
Erica scoparia	4			
Calluna vulgaris	1	4		
Ulex nanus		4		
Erica scoparia		4		
Erica cinerea		3		
Erica ciliaris		2		
Rhamnus frangula	1	1		
Molinia caerulea			4	
Agrostis curtisii			2	
Quercus robur			1	
Pteridium aquilinum			1	
Potentilla tormentilla			1	
Hypnum ericetorum				4
Pseudoscleropodium purum				1
Dicranum scoparium				1
Pleurozium schreberi				1